Electronic Supplementary Information

Non-covalent interactions in electrochemical reactions and implications in clean energy applications

Botao Huang*[a,b], Sokseiha Muy[a,c], Shuting Feng[a,d], Yu Katayama[a,e], Yi-Chun Lu[f], Gang Chen[g] and Yang Shao-Horn*[a,b,c,g]

[a] Electrochemical Energy Laboratory, Massachusetts Institute of Technology, 77 Massachusetts Avenue, Cambridge, MA 02139, USA
[b] Research Laboratory of Electronics, Massachusetts Institute of Technology, 77 Massachusetts Avenue, Cambridge, MA 02139, USA
[c] Department of Material Science and Engineering, Massachusetts Institute of Technology, 77 Massachusetts Avenue, Cambridge, MA 02139, USA
[d] Department of Chemical Engineering, Massachusetts Institute of Technology, 77 Massachusetts Avenue, Cambridge, MA 02139, USA
[e] Department of Applied Chemistry, Graduate School of Sciences and Technology for Innovation, Yamaguchi University, Ube 755-8611, Japan
[f] Electrochemical Energy and Interfaces Laboratory, Department of Mechanical and Automation Engineering, The Chinese University of Hong Kong, Shatin, N.T. 999077, Hong Kong SAR, China
[g] Department of Mechanical Engineering, Massachusetts Institute of Technology, 77 Massachusetts Avenue, Cambridge, MA 02139, USA

* **Corresponding authors**
Email: huang73@mit.edu
Email: shaohorn@mit.edu

Table of contents

Electronic Supplementary Information 1: Proposed solvation model of redox center

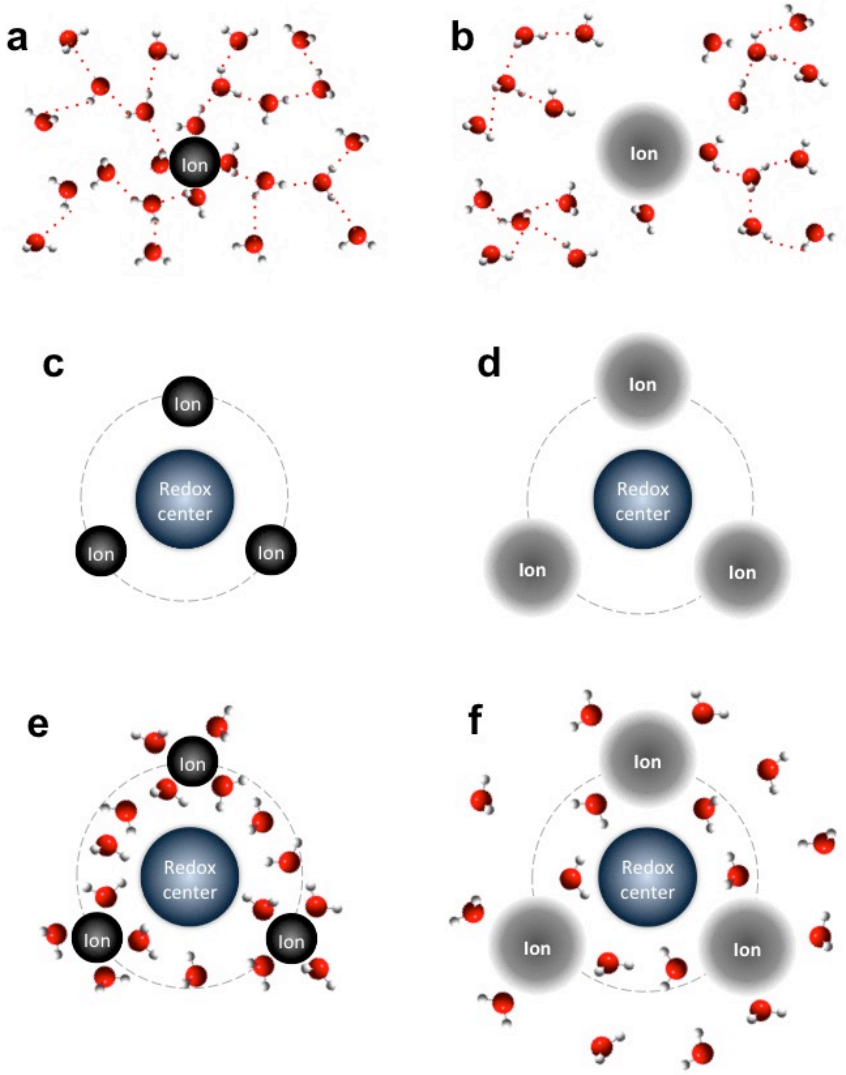

Figure S1. Proposed models taking account into non-covalent interactions among redox center/inert ions/water molecules within the solvaion shell of redox couples. a) structure making ions enhance HB network in liquid water; b) structure breaking ions weaken HB in bulk water; c) and d) redox centre attracts ions with opposite sign of charge to form a new ionic atmosphere; e) structure making ions make more order of water molecules in the solvation shell of redox center; f) structure breaking ions make more disorder of water molecules in the solvation shell of redox center.

Electronic Supplementary Information 2: Stability of $[Fe(H_2O)_6]^{3+/2+}$ and $[Fe(CN)_6]^{3-/4-}$ in the presence of perchlorate salts

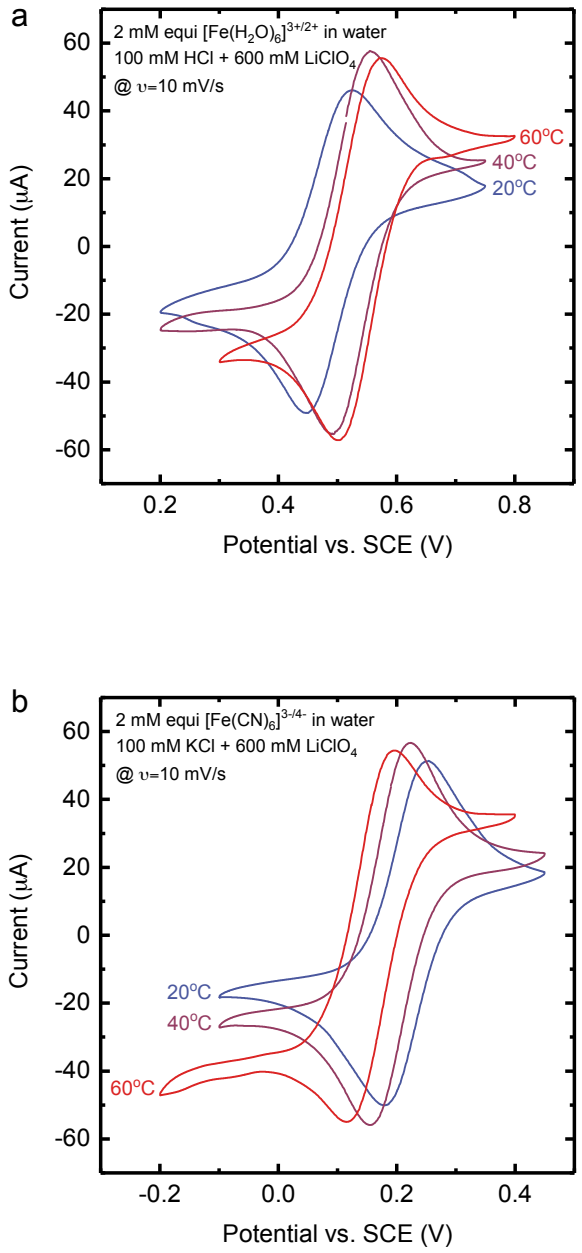

Figure S2. Cyclic voltammograms of a) $[Fe(H_2O)_6]^{3+/2+}$ and b) $[Fe(CN)_6]^{3-/4-}$ at 20 °C, 40 °C and 60°C, measured in aqueous electrolyte containing 2 mM equimolar of redox couple and 0.6 M $LiClO_4$.

Electronic Supplementary Information 3: Electrochemical measurement set-up and procedure

Electrochemical measurements were performed with a Biologic SP-300 potentiostat in an isothermal three-electrode electrochemical system under Ar atmosphere (Figure S3). The working electrode (WE) is a platinum (Pt) rotating disc electrode (RDE) (Pine instrument). Potentials are referenced to a saturated calomel electrode (SCE). Steady-state open circuit voltage (OCV) of WE was measured at 1600 rpm. Electrical impedance spectroscopy (EIS) measurement was carried out at the OCV for frequency 20 kHz-100 mHz with an amplitude of 10 mV. To estimate exchange current density, cyclic voltammetry (CV) scans were performed at sweep rate 10 mV s^{-1} and rotation rate at 1600 rpm. Potentials were corrected for the ohmic resistance from the high frequency intercept of the real impedance, and the forward and reverse scans were averaged. The values of exchange current density were obtained by fitting cyclic voltammograms to the Butler-Volmer equation. For the temperature dependent measurements, the temperature of the electrochemical cell was controlled by a thermal bath circulator (Thermo Neslab RTE 7).

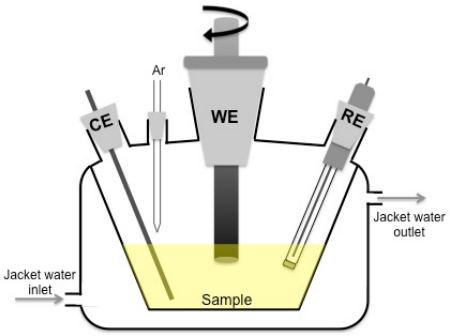

Figure S3. Isothermal cell for electrochemical measurements.

Electronic Supplementary Information 4: Reaction entropy and temperature coefficient of redox couples

The redox reaction entropyΔs can be estimated by the temperature dependence of the formal potential $E^{0\prime}$ of the redox couple:

$$\Delta S = nF\frac{dE^{0\prime}(T)}{dT}$$

F is the Faraday constant and n is the number of electrons involved in the corresponding redox process. The ratio $dE^{0\prime}/dT$ is also called the temperature coefficient of the redox couples, denoted by α:

$$\alpha = \frac{dE^{0\prime}(T)}{dT}$$

In an isothermal electrochemical cell (Figure S3), potentials are referenced to a saturated calomel electrode (SCE), thus:

$$E^{0\prime}(T) = E_{meas}(T) + E_{SCE}(T)$$

$E_{meas}(T)$ is the measured potential at the working electrode (WE); $E_{SCE}(T)$ is the potential of SCE at temperature T. Then, the redox reaction entropy Δs can be expressed as,

$$\Delta S = nF\left[\frac{dE_{meas}(T)}{dT} + \frac{dE_{SCE}(T)}{dT}\right] = nF(\alpha_{meas} + \alpha_{SCE})$$

The calibration of the temperature coefficient of SCE is shown in Electronic Supplementary Information 6.try2ehj/

Electronic Supplementary Information 5: Formal potentials by open circuit voltage (OCV)

According to Nernst equation, the electrode potential at open circuit voltage (OCV) can be written as:

$$E_{OCV} = E^0 + \frac{RT}{nF}ln\frac{a_{Ox}}{a_{Red}}$$

E^0 denotes the standard potential of redox couples. The activity a_i of specie i can be expressed as the product of activity coefficient γ_i and concentration C_i:

$$a_i = \gamma_i \cdot C_i$$

Thus, we have,

$$E_{OCV} = E^0 + \frac{RT}{nF} ln \frac{\gamma_{Ox}}{\gamma_{Red}} + \frac{RT}{nF} ln \frac{C_{Ox}}{C_{Red}}$$

In this work, all electrolytes contains equimolar redox species, thus, the measured OCV corresponds to the formal potential of redox couples:

$$E_{OCV} = E^{0\prime} = E^0 + \frac{RT}{nF} ln \frac{\gamma_{Ox}}{\gamma_{Red}}$$

The formal potentials of $[Fe(CN)_6]^{3-/4-}$ and $[Fe(H_2O)_6]^{2+/3+}$ depend linearly upon temperature, as shown in Figure S4.

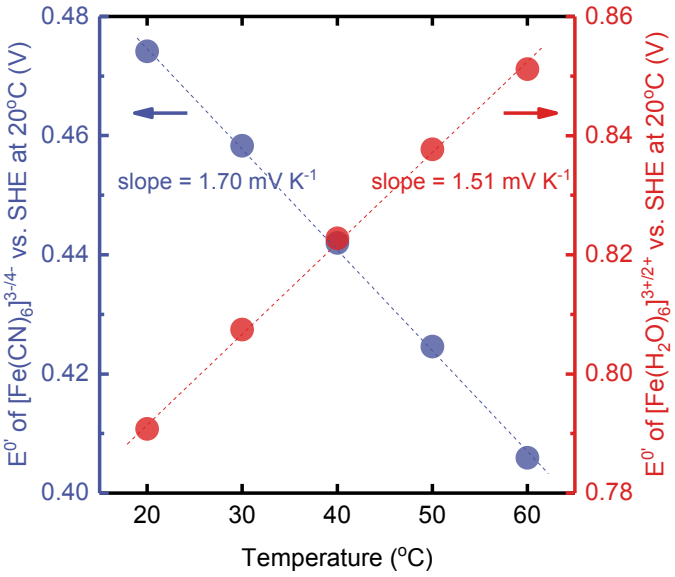

Figure S4. The linear variation of the formal potentials of $[Fe(CN)_6]^{3-/4-}$ and $[Fe(H_2O)_6]^{3+/2+}$ for the temperature range between 20 and 60°C. OCV measured in aqueous electrolytes contains 2 mM equimolar of the redox couple.

Electronic Supplementary Information 6: Temperature coefficient of SCE reference electrode

The temperature coefficient of the saturated calomel electrode (SCE) was calibrated using a non-isothermal cell set-up (Figure S5). Two independently thermostated cells (cell 1 and 2) were filled with 4 M KCl electrolyte and connected by a 4 M KCl salt bridge. Two identical SCE were used and inserted in the cells. For calibrating RE2, the change of the electromotive force $dE_{SCE}(T)$ between RE2 and RE1 upon an increase of temperature difference at the two compartments was measured (the temperature of cell 1 was maintained at 22°C whereas that of cell 2 increased from 20°C to 60°C by an increment of 10°C). The temperature coefficient of the SCE corresponds to the slope of the plot of $dE_{SCE}(T)$ against dT, approximately 0.3 mV K^{-1} as shown in Figure S6.

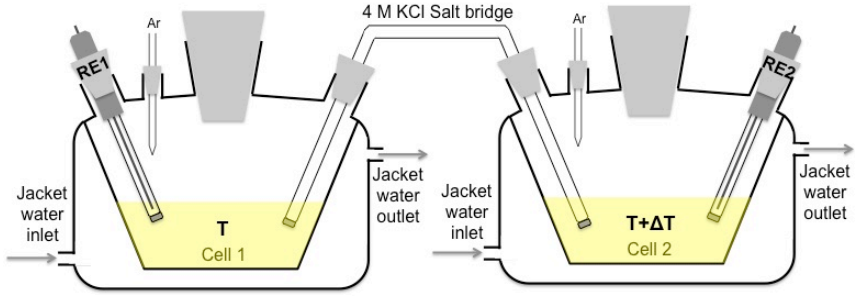

Figure S5. Non-isothermal cell for SCE temperature coefficient calibration

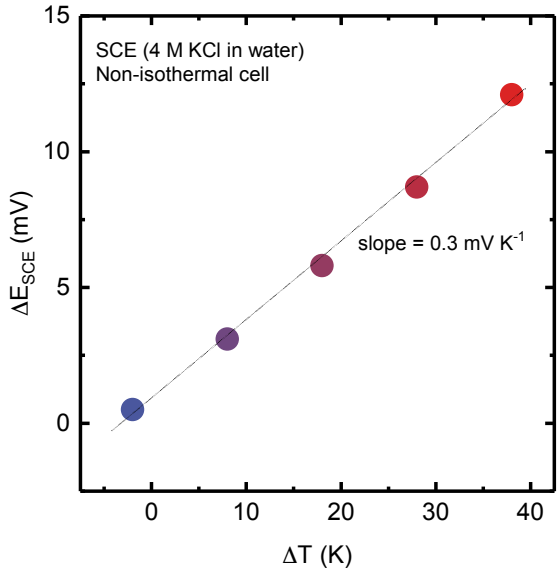

Figure S6. Calibration curve of the temperature coefficient of SCE reference electrode.

Electronic Supplementary Information 7: Error bar of reaction entropy measurements

The error bar of reaction entropy measurements was estimated based on ten independently repeated measurements. The values of error bar were estimated to be less than 2%. For example, figure S7 shows ten independently repeated reaction entropy measurements of 2 mM ferro/ferricyanide $[Fe(CN)_6]^{3-/4-}$ aqueous solution; the average value was 179.3 J mol^{-1} K^{-1} with an error bar of 2.3 J mol^{-1} K^{-1}.

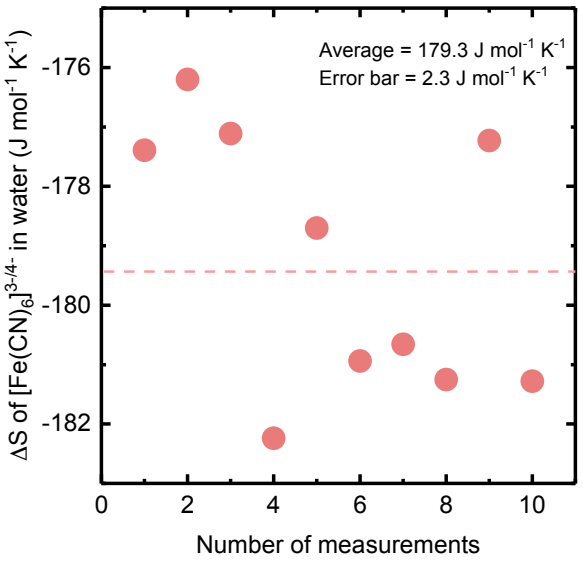

Figure S7. An example of the determination of the average value and the error bar of the reaction entropy measurements: Ten independently repeated reaction entropy measurements of 2 mM ferro/ferricyanide $[Fe(CN)_6]^{3-/4-}$ aqueous solution.

Electronic Supplementary Information 8: Determination of exchange current density i_0 from Butler-Volmer equation

To estimate the exchange current density, cyclic voltammetry (CV) scans were performed at sweep rate 10 mV s^{-1} and at 1600 rpm rotation. Potentials were corrected for the ohmic resistance from the high frequency intercept of the real impedance, and the forward and reverse scans were averaged. To extract exchange current density i_0, cyclic voltammograms for overpotential η ranging between -0.03 V and 0.03 V have been fitted to the Butler-Volmer equation:

$$\mathrm{i} = i_0 \left[exp\left(\frac{\alpha F}{RT}\eta\right) - exp\left(-\frac{(1-\alpha)F}{RT}\eta\right)\right]$$

with charge transfer coefficient α=0.5, faraday constant F=96485 C mol^{-1}, idea gas constant R=8.314 J mol^{-1} K^{-1} and temperature T=293.15 K.

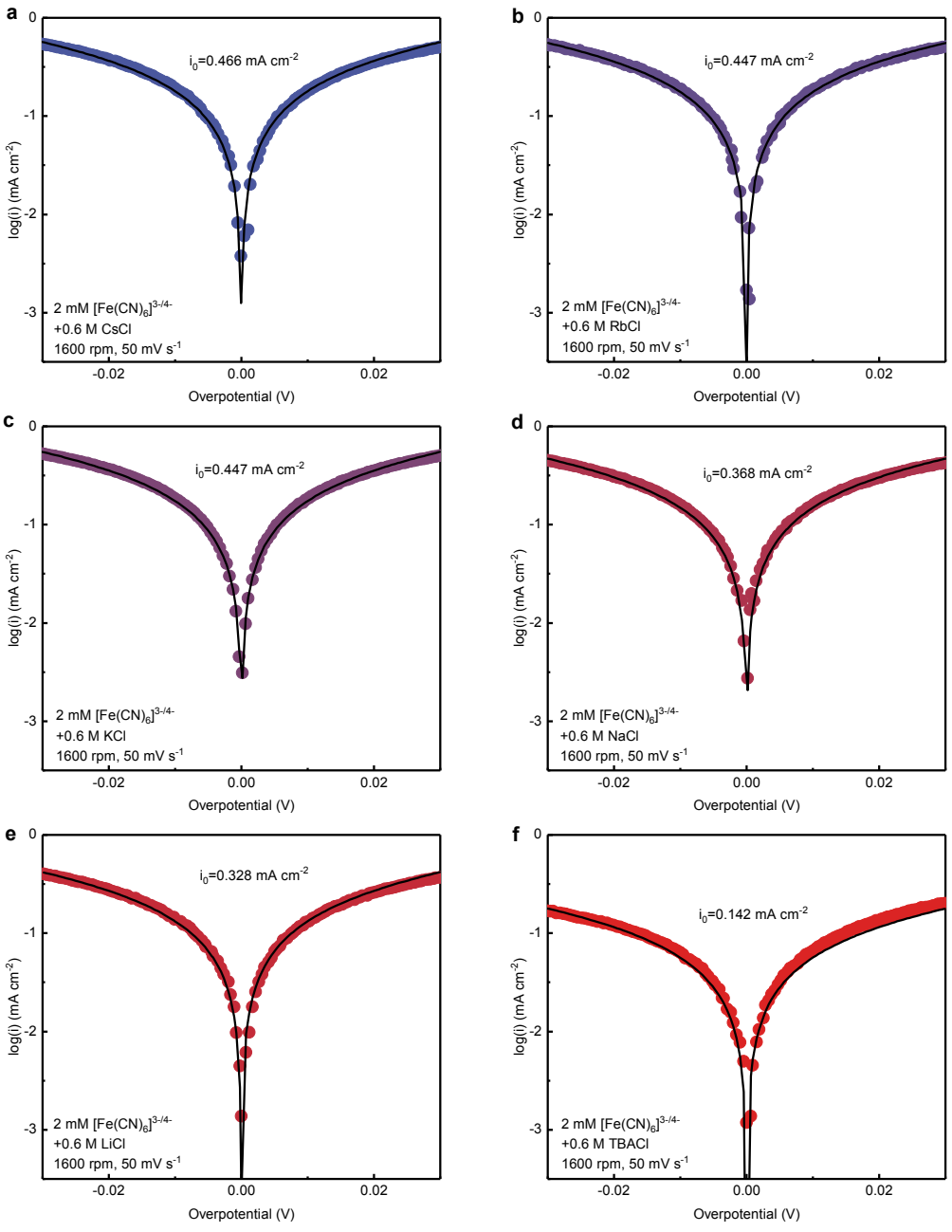

Figure S8. Tafel plot of cyclic votammograms recorded in electrolytes containing 2 mM $[Fe(CN)_6]^{3-/4-}$ and 0.6 M chloride salt supporting electrolyte at 20°C and fitting to the Butler-Volmer equation: a) CsCl, b) RbCl, c) KCl, d) NaCl, e) LiCl and f) TBACl.

Electronic Supplementary Information 9: Additional information for DFT methods.

Ab-initio molecular dynamics (AIMD) simulations were performed on the system containing 93 water molecules and one ferricyanide $[Fe(CN)_6]^{3-}$ anion as well as 3 cations to make the overall system electrically neutral. The size of the unit cell for each system was decided based on the aqueous solution density and the size of the cations

Cation	Coordination number of cation[1] (-)	Shannon radius of cation [2] (Å)	Volume of cation (Å^3)	Unit volume (Å^3)	Unit cell size (Å)
Li^+	4	0.59	0.86	2515.46	13.60
Na^+	5	1	4.19	2525.44	13.62
K^+	6	1.38	11.01	2545.90	13.66
Rb^+	7	1.56	15.90	2560.58	13.72
Cs^+	9	1.78	23.62	2583.75	13.66

Table S1. The coordination number, Shannon radius volume of cations and unit cell size for each DFT system.

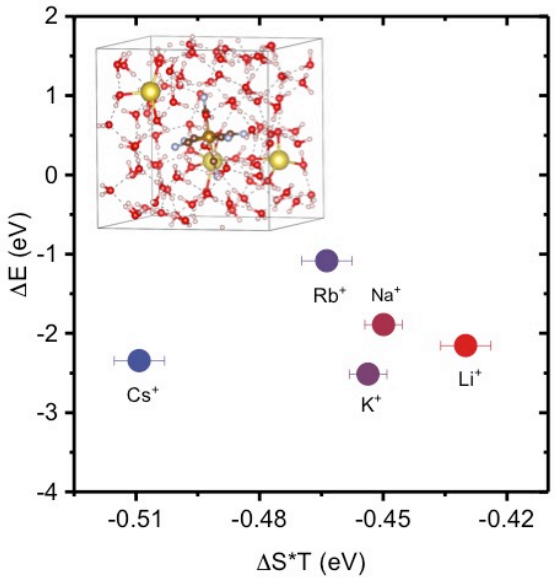

Figure S9. The computed energy of ferri/ferrocyanide redox surrounded by cations and water molecules by DFT plotted against experimentally measured redox entropy. The Gibbs energy of ferri/ferrocyanide $[Fe(CN)_6]^{3-/4-}$ redox is estimated by $\Delta E = E\left(Fe(CN)_6{}^{4-}\right) - E\left(Fe(CN)_6{}^{3-}\right)$, where $E\left(Fe(CN)_6{}^{3-}\right)$ is the single point energy computed using the Gaussian 09 computational package[3] and the optimized structure of the system containing $[Fe(CN)_6]^{3-}$, 3 cations and 93 water

molecules obtained using VASP. $E(Fe(CN)_6^{4-})$ is the single point energy of the corresponding system containing $[Fe(CN)_6]^{4-}$ calculated upon adding one electron to the optimized geometry of the system containing $[Fe(CN)_6]^{3-}$. The single point energy calculations were performed at the B3LYP[4,5] level of theory. The 6-31G(d,p) basis set was used for all atoms except for Rb and Cs, which were computed using the LANL2DZ pseudo-potential. The inset shows the unit cell of the simulation containing 93 water molecules, one ferricyanide anion and 3 cations (Li^+, Na^+, K^+, Rb^+ or Cs^+).

Electronic Supplementary Information 10: Additional data of reaction entropy measurement of $[Fe(H_2O)_6]^{3+/2+}$ and $[Fe(CN)_6]^{3-/4-}$ couples in the presence of different supporting electrolytes.

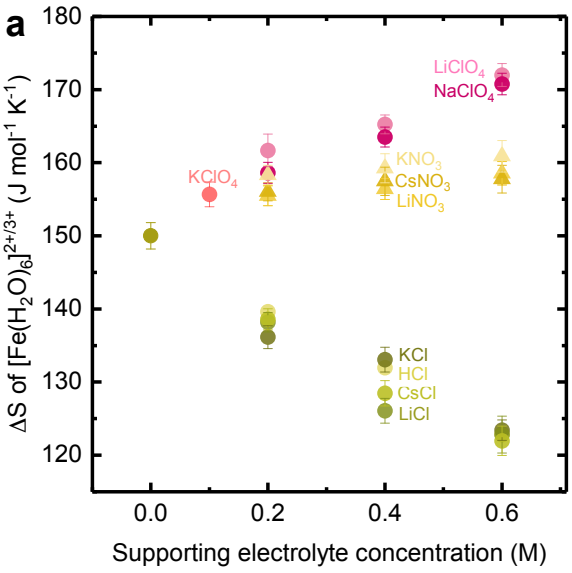

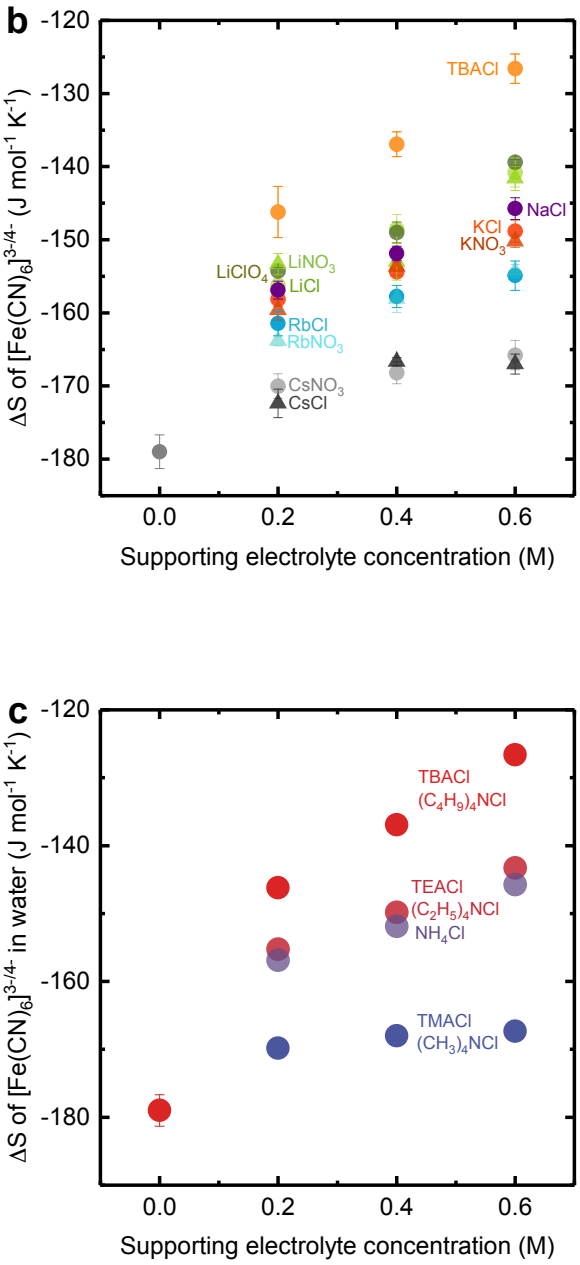

Figure S10. The dependence of the reaction entropy of a) $[Fe(H_2O)_6]^{3+/2+}$ and b) $[Fe(CN)_6]^{3-/4-}$ in 2 mM aqueous solution upon the nature and concentration of the supporting electrolytes (alkali salt). c) The influence of tetramethylammonium chloride (TMACl), tetraethylammonium chloride (TEACl) and tetrabuthylammonium chloride (TBACl) on the reaction entropy of 2 mM equimolar $[Fe(CN)_6]^{3-/4-}$ in aqueous solution.

Salts	$NiCl_2$	$Mg(NO_3)_2$	$CaCl_2$	$CoCl_2$
ΔS (@0.6M salt) (J mol^{-1} K^{-1})	90.03	109.91	127.01	89.13

Table S2. Summary of the reaction entropy values of 2 mM equimolar aqueous solution of $[Fe(CN)_6]^{3-/4-}$ in the presence of 0.6 M divalent salts.

Electronic Supplementary Information 11: The dependence of the reaction entropy of $[Ag(H_2O)_4]^{+/0}$ upon nitrate and perchlorate supporting electrolytes.

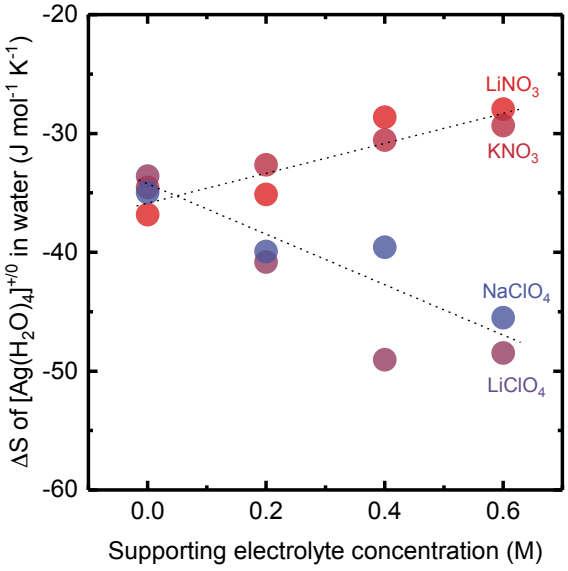

Figure S11. The dependence of reaction entropy of $[Ag(H_2O)_4]^{+/0}$ upon the nature and concentration of nitrate and perchlorate supporting electrolytes.

Electronic Supplementary Information 12: FT-IR spectroscopy results

The Fourier transform infrared (FT-IR) spectra of electrolytes were obtained on an FT-IR Vertex 70 (Bruker). The measurements were performed with a 1 cm^{-1} resolution in the 4000-1000 cm^{-1} spectral range; 256 scans were averaged. The FT-IR spectra were recorded using a single reflection ATR accessory (Pike Vee-Max II, Pike Technologies) with a Si prism (Pier optics) at an incident angle of 45 degrees.

In aqueous solution, CN ligand of ferro-/ferricyanide anions could be influenced by their surrounding environment: CN/metal center, CN/cations and CN/water molecules. Figure S12.1a) shows the influence of metal center on the wavenumber of CN stretching. Due to strong interaction between CN groups and metal center via covalent bond, CN stretching wavenumber shifts significantly to a lower value for 0.2 M $K_4Fe(CN)_6$ solution (2037 cm^{-1}) compared to 0.2 M $K_4Pt(CN)_6$ solution (2148 cm^{-1}). Then, CN stretching features of 0.2 M $K_4Fe(CN)_6$ in water (H_2O) and heavy water (D_2O) were compared in Figure S12.1b). CN stretching peak shifts 1 cm^{-1} when $[Fe(CN)_6]^{4-}$ anions are transferred from water to heavy water. This behavior indicates that $[Fe(CN)_6]^{4-}$ anions interact with water molecules nearby, probably in their solvation shell, and that could be probed by FT-IR. To probe the effect of CN/inert ion interaction, CN stretching features of 0.2 M $K_4Fe(CN)_6$ (2038.8 cm^{-1}) and 0.2 M $Na_4Fe(CN)_6$ (2037.5 cm^{-1}) in water were compared (Figure S13.1c). Although the molar masses of Na^+ (23 g mol^{-1}) and K^+ (39 g mol^{-1}) are significantly different, the difference between CN stretching peak value of the two cases was only 1.3 cm^{-1}, suggesting that the wavenumber shift is likely due to the change in CN/water interaction induced by the inert ions.

To reveal the influence of cations on the water structure change of $[Fe(CN)_6]^{4-}$ anion solvation shell, the CN stretching of aqueous solutions of 0.2 M $K_4Fe(CN)_6$ in the presence of 0.8 M chloride salt for different cations was then studied. Figure S12.2 shows that CN stretching peaks shift to lower wavenumber from structure breaking ions to structure making ions ($Cs^+ > Rb^+ > K^+ > Na^+ > Li^+ > TBA^+$), likely due to the change of water molecule arrangement within the solvation shell in the presence of different cations. FT-IR results are consistent with Raman results shown in the main text.

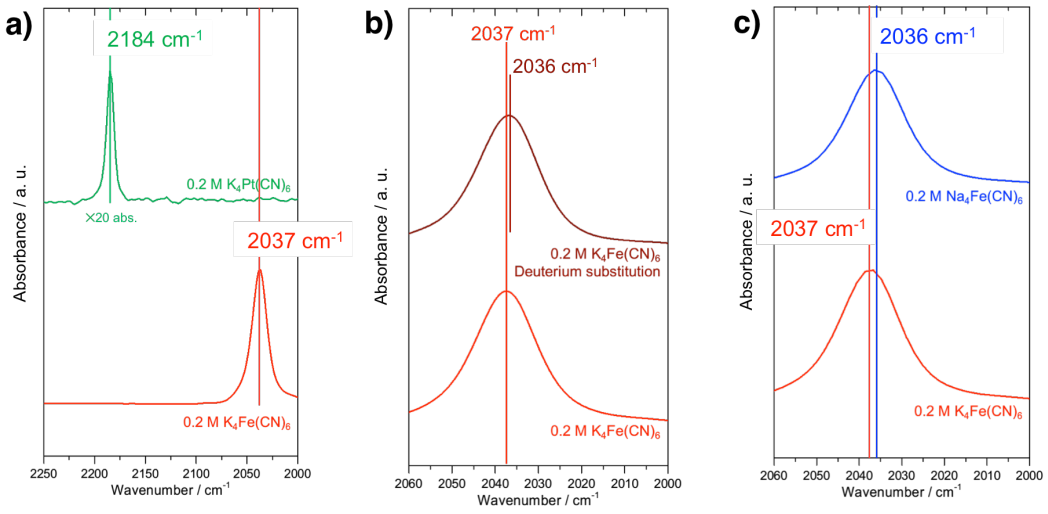

Figure S12.1 FT-IR spectra of CN stretching for probing interaction between $[Fe(CN)_6]^{4-}$ anion species and surrounding environment. a) 0.2 M $K_4Fe(CN)_6$ and 0.2 M $K_4Pt(CN)_6$ in water; b) 0.2 M $K_4Fe(CN)_6$ in water and heavy water; c) 0.2 M $K_4Fe(CN)_6$ and 0.2 M $Na_4Fe(CN)_6$ in water.

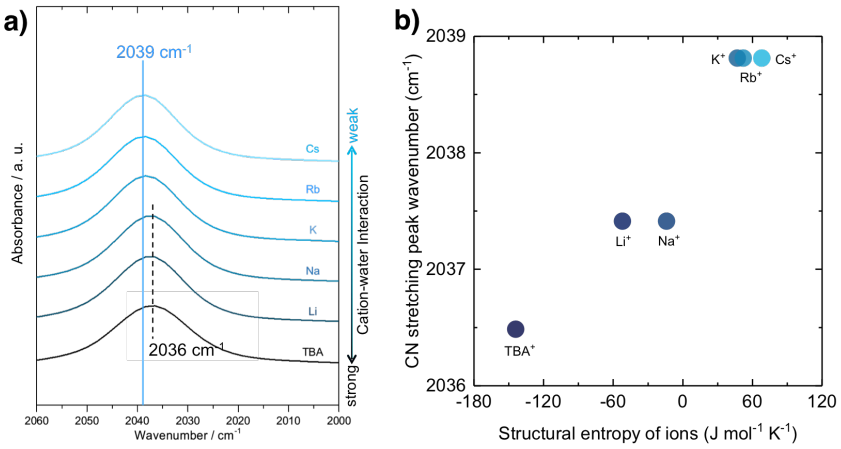

Figure S12.2 Probing water structure change of $[Fe(CN)_6]^{4-}$ anion solvation shell due to the presence of cations. a) FT-IR spectra of CN stretching of electrolytes containing 0.2 M $K_4Fe(CN)_6$ and 0.8 M chloride salts (CsCl, RbCl, KCl, NaCl, LiCl and TBACl) in water.

References

1 Y. Marcus, *Chem. Rev.*, 2009, **109**, 1346–1370.
2 R. Shannon, *Acta Crystallographica Section A*, 1976, **32**, 751–767.
3 M. J. Frisch, G. W. Trucks, H. B. Schlegel, G. E. Scuseria, M. A. Robb, J. R. Cheeseman, R. Gomperts, B. Mennucci, H. P. Hratchian, J. V. Ortiz and A. F. Izmaylov, .
4 A. D. Becke, *The Journal of Chemical Physics*, 1993, **98**, 5648–5652.
5 C. Lee, W. Yang and R. G. Parr, *Phys. Rev. B*, 1988, **37**, 785–789.